# Structure and Bonding in Dinuclear Oxoanions of V, Nb, Ta, Mo, and W

**Adam J. Bridgeman*,† and Germán Cavigliasso†,‡**

*Department of Chemistry, University of Hull, Kingston upon Hull, HU6 7RX, U.K., and Department of Chemistry, University of Cambridge, Lensfield Road, Cambridge CB2 1EW, U.K.*

*Received: March 8, 2001; In Final Form: May 21, 2001*

The structure and bonding in $[M_2O_7]^{n-}$ anions of the early transition metals V, Nb, Ta, Mo, and W have been investigated by density-functional methods. Several molecular conformations have been tested in geometry optimizations, and systems with a linear M−O−M bridge have been the only structures obtained for V, Nb, and Ta, and the most stable configurations for Mo and W. Molecular-orbital analysis has indicated that multiple bonds are formed between the metal and both bridging ($O_b$) and terminal ($O_t$) oxygen atoms. However, it has been found that M−$O_b$ interactions are characterized by bond lengths and bond orders that are typical of a single M−O bond. The results from population analysis (Mulliken charges and Mayer bond indices) have suggested that the repulsive interactions between the ends of the molecules may be a more important structural factor in determining the configuration of the bridge than M−$O_b$ $\pi$ bonding is.

## Introduction

Vanadium, molybdenum, tungsten, and to a lesser extent niobium and tantalum stand out among the transition metals in their ability to form polymeric oxoanions. These polyoxoanions or polyoxometalates constitute an immense class of compounds in number and diversity[1,2] and exhibit remarkable chemical and physical properties, their actual and potential applications spanning a variety of fields, including medicine, catalysis, solid-state technology, and chemical analysis.[2−4]

The structures of polyoxometalates can be characterized as an assemblage of $MO_x$ coordination polyhedra, the octahedron being the most commonly observed constituent unit.[1] However, the simplest polyoxoanions, namely the dinuclear $[M_2O_7]^{n-}$ species, consist of two corner-sharing tetrahedra, and therefore contain only four-coordinate metal centers.

The existence of discrete $[M_2O_7]^{n-}$ anions has been experimentally confirmed only for V[5,6] and Mo,[7−9] among the polyanion-forming transition metals, but unlike the case of the larger polyoxometalates, it is not limited to these elements. The Cr species, $[Cr_2O_7]^{2-}$, is arguably the best known dinuclear oxoanion, and crystal structures for several main-group systems have also been reported.[10,11]

Although computational studies of transition-metal $[M_2O_7]^{n-}$ anions have concentrated on dichromate,[12−14] some calculations on the V, Nb, Ta, Mo, and W systems have been reported.[12,15,16] Considerable attention has been focused on the molecular structures of the oxoanions, as experimental data for crystals have revealed a diversity of conformations in the solid state. Also, investigations of the vibrational[12,16] and electronic[12] spectra of some species have been performed. Notably, descriptions of the chemical bonding in these anions (based on computational results) are scarce and, to the best of our knowledge, limited to a Mulliken population and density analysis of $[Mo_2O_7]^{2-}$ and $[W_2O_7]^{2-}$ [12] and a discussion of the importance of d−p orbital interactions in determining the preferred geometry of the M−O−M bridging unit.[16]

In the present work, the results of density-functional investigations on $[V_2O_7]^{4-}$ $[Nb_2O_7]^{4-}$ $[Ta_2O_7]^{4-}$ $[Mo_2O_7]^{2-}$, and $[W_2O_7]^{2-}$ are reported. The optimized molecular geometry of the oxoanions is utilized to assess the performance of the computational methods employed, and a detailed account of the nature of the M−O chemical bonds, based on molecular-orbital and population analyses including bond-order indices, is presented.

## Computational Approach

The density-functional (DF) calculations reported in this work were performed with the ADF[17] density-functional code and with the GAMESS-UK[18] suite of quantum chemistry programs. Functionals based on the Vosko−Wilk−Nusair (VWN)[19] form of the local density approximation (LDA),[20] and on a combination (BP86) of Becke's 1988 exchange[21] and Perdew's 1986 correlation[22] corrections to the LDA, and basis sets of triple-$\zeta$ (tz) quality incorporating frozen cores and the ZORA relativistic approach[17] were utilized in ADF calculations. The B3LYP[23] functional and basis sets of double-$\zeta$ (dz) quality and of the effective-core-potential[24−26] type were employed in GAMESS-UK calculations. Bond indices were obtained according to Mayer's definition,[27,28] with a program[29] designed for their calculation from the ADF output file. Molecular-orbital graphics were generated with the MOLDEN program.[30]

## Results and Discussion

**Molecular Structures.** Geometry optimizations of conformations with $D_{3h}$, $C_{2v}$ (syn and anti), $D_{3d}$, $C_s$, and $C_2$ symmetry (Figure 1) were performed for all five $[M_2O_7]^{n-}$ systems. The relative total energies of the conformers are given in Table 1, and a comparison of calculated and (available) experimental values for the structural parameters is presented in Tables 2 and 3. It should be noted that the results of the present calculations correspond to isolated molecules and do not include any solid-state effects. However, data for the anions are only available from studies of crystalline phases.

* Corresponding author. Telephone: +44 1482 466549. Facsimile: +44 1482 466410. E-mail: A. J.Bridgeman@chem.hull.ac.uk.
† University of Hull.
‡ University of Cambridge.

10.1021/jp010894p CCC: $20.00 
Published on Web 06/28/2001

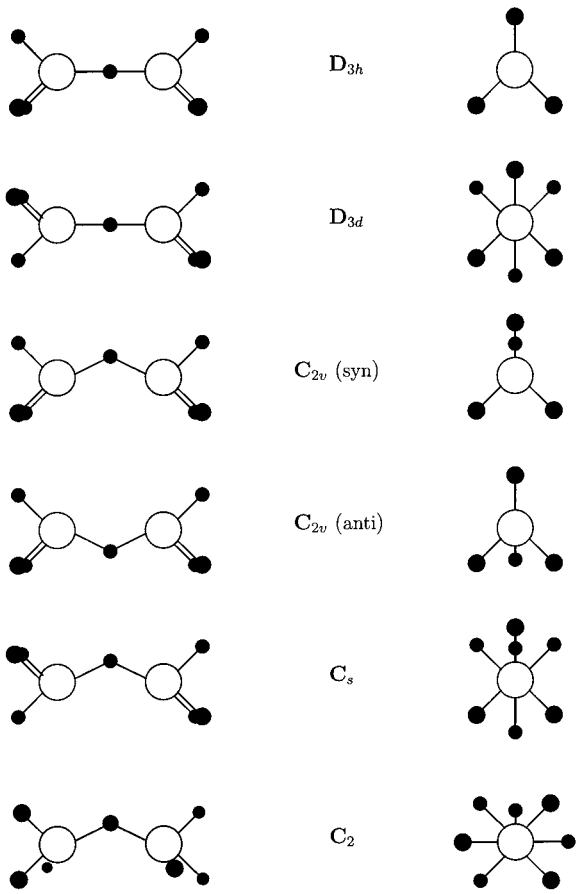


**Figure 1.** Structural schemes (left) for $[M_2O_7]^{n-}$ conformers (M: open circle; O: full circle) and projections (right) along the M−M axis.

**TABLE 1: Relative Total Energies (kJ mol$^{-1}$) of Optimized Molecular Structures[a]**

| molecule | symmetry | LDA | B3LYP |
|---|---|---|---|
| $[V_2O_7]^{4-}$ | $D_{3d}$ | 0.00 | 0.00 |
| | $D_{3h}$ | 1.03 | 1.92 |
| $[Nb_2O_7]^{4-}$ | $D_{3d}$ | 0.00 | 0.00 |
| | $D_{3h}$ | 0.85 | 2.90 |
| $[Ta_2O_7]^{4-}$ | $D_{3d}$ | 0.00 | 0.00 |
| | $D_{3h}$ | 1.20 | 2.27 |
| $[Mo_2O_7]^{2-}$ | $D_{3d}$ | 0.00 | 0.00 |
| | $D_{3h}$ | 0.35 | 1.44 |
| | $C_{2v,\mathrm{anti}}$ | 1.04 | 3.70 |
| | $C_2$ | 1.45 | 5.21 |
| | $C_s$ | 1.83 | 4.27 |
| | $C_{2v,\mathrm{syn}}$ | 2.46 | 8.68 |
| $[W_2O_7]^{2-}$ | $D_{3d}$ | 0.00 | 0.00 |
| | $D_{3h}$ | 0.26 | 1.15 |
| | $C_{2v,\mathrm{anti}}$ | 1.28 | 3.54 |
| | $C_2$ | 1.74 | 4.90 |
| | $C_s$ | 1.85 | 4.68 |
| | $C_{2v,\mathrm{syn}}$ | 2.64 | 7.81 |

[a] The most stable conformer was chosen as reference.

Three different density-functional approaches were utilized for the geometry optimizations of the $D_{3d}$ and $D_{3h}$ conformers. Although a direct comparison of calculation and experiment is not possible due to the aforementioned discrepancies, it is observed that (where experimental information is available) the LDA results are, in general, more satisfactory than those obtained with BP86 and B3LYP methods, the bond lengths from LDA calculations being closest to the crystal-structure parameters. In species with relatively high negative charges, bond distances predicted by gas-phase calculations can be expected to be longer than the corresponding solid-state values, and in these cases the well-known overbinding character of the LDA[31] may introduce some favorable cancellation, and therefore, better geometries (than those yielded by more elaborate functionals) can be obtained, as shown by the present results and also by recent work on main-group and transition-metal $[MO_4]^{n-}$ anions.[32]

**TABLE 2: Structural Parameters (M−O Distances in Picometers, M−O−M and O−M−O Angles in Degrees) for the Species with Linear M−O−M Units**

| molecule | parameter | LDA | BP86 | B3LYP | experiment |
|---|---|---|---|---|---|
| $[V_2O_7]^{4-}$ | $M-O_b$ | 186 | 190 | 188 | 176−182[35−37] |
| | $M-O_t$ | 171 | 173 | 171 | 165−172 |
| | $O_t-M-O_b$ | 111 | 111 | 111 | 104−110 |
| | $O_t-M-O_t$ | 108 | 108 | 108 | 110−113 |
| $[Nb_2O_7]^{4-}$ | $M-O_b$ | 200 | 204 | 203 | |
| | $M-O_t$ | 185 | 187 | 186 | |
| | $O_t-M-O_b$ | 111 | 111 | 111 | |
| | $O_t-M-O_t$ | 108 | 108 | 108 | |
| $[Ta_2O_7]^{4-}$ | $M-O_b$ | 200 | 202 | 201 | |
| | $M-O_t$ | 186 | 189 | 186 | |
| | $O_t-M-O_b$ | 111 | 111 | 111 | |
| | $O_t-M-O_t$ | 108 | 108 | 108 | |
| $[Mo_2O_7]^{2-}$ | $M-O_b$ | 190 | 193 | 193 | 184[9] |
| | $M-O_t$ | 175 | 177 | 176 | 169−170 |
| | $O_t-M-O_b$ | 110 | 110 | 110 | 109−110 |
| | $O_t-M-O_t$ | 109 | 109 | 109 | 109−110 |
| $[W_2O_7]^{2-}$ | $M-O_b$ | 191 | 193 | 193 | |
| | $M-O_t$ | 177 | 179 | 176 | |
| | $O_t-M-O_b$ | 110 | 110 | 110 | |
| | $O_t-M-O_t$ | 109 | 109 | 109 | |

**TABLE 3: Structural Parameters (M−O Distances in Picometers, M−O−M and O−M−O Angles in Degrees) for the Species with Bent M−O−M Units**

| molecule | parameter | | LDA | experiment |
|---|---|---|---|---|
| $[Mo_2O_7]^{2-}$ | $M-O_b$ | | 191 | 182−195[7,8] |
| | $M-O_t$ | | 175 | 168−179 |
| | $O_t-M-O_b$ | | 110 | 109−110 |
| | $O_t-M-O_t$ | | 109 | 109−110 |
| | M−O−M | $C_{2v,\mathrm{anti}}$ | 161 | |
| | | $C_{2v,\mathrm{syn}}$ | 152 | |
| | | $C_2$ | 154 | 154 |
| | | $C_s$ | 153 | 160 |
| $[W_2O_7]^{2-}$ | $M-O_b$ | | 191 | |
| | $M-O_t$ | | 177 | |
| | $O_t-M-O_b$ | | 110 | |
| | $O_t-M-O_t$ | | 108 | |
| | M−O−M | $C_{2v,\mathrm{anti}}$ | 163 | |
| | | $C_{2v,\mathrm{syn}}$ | 154 | |
| | | $C_2$ | 156 | |
| | | $C_s$ | 154 | |

In view of the results for $D_{3d}$ and $D_{3h}$ conformations, only LDA optimizations were carried out on the systems with bent M−O−M bridging units, and the vast majority of the results reported throughout this work are based on LDA/tz calculations. Nevertheless, because the LDA is known to be not as reliable for thermochemistry as the B3LYP functional is,[31] relative energies have also been determined by performing single-point B3LYP calculations at LDA geometries. It is worth noting that, although the differences are quantitatively significant (as expected), the agreement between LDA and B3LYP calculations is remarkably good on a qualitative basis, given the considerably small energies involved.

For the systems with the highest negative charge ($[V_2O_7]^{4-}$, $[Nb_2O_7]^{4-}$, $[Ta_2O_7]^{4-}$), only structures containing a linear M−O−M moiety were obtained (optimizations that were started from a $C_2$, $C_{2v}$, or $C_s$ conformation converged to a $D_{3h}$ or $D_{3d}$ configuration), and the staggered conformation was found to

be slightly more stable. Although diniobate and ditantalate species have not been prepared, several experimental studies of divanadates have reported structures of $D_{3d}$ symmetry (nevertheless, the M−O−M angle values observed in crystals span a considerably wide range, V−O−V: 117−180° [5,6]). The results of the present work agree with those of previous Hartree−Fock (HF) and DF[16] calculations of the V, Nb, and Ta dimetalate ions, which have also yielded, exclusively, the $D_{3d}$ and $D_{3h}$ conformers.

In the case of $[Mo_2O_7]^{2-}$ and $[W_2O_7]^{2-}$, the geometry optimizations for all six molecular conformations investigated were successful. The results in Table 1 indicate that, although dimolybdates and ditungstates with a linear M−O−M unit should be more stable than those possessing a bent bridge, the differences are too small for definitive conclusions to be drawn. Moreover, these results do not agree completely with previously reported DF calculations,[16] which have also shown similarly small differences in the relative stabilities of the conformers but have suggested that the systems with a bent M−O−M moiety should be the most stable structures. As in the Nb and Ta cases, discrete ditungstate molecules are not known. However, materials containing $[Mo_2O_7]^{2-}$ ions with $D_{3d}$,[9] $C_2$,[7] and $C_s$[8] configurations have been synthesized.

For the V and Mo systems, where experimental data are available, the calculated geometry for the isolated molecules compares reasonably well with the parameters from the crystal structures. In general, M−O−M and O−M−O angles and terminal-bond distances are closely reproduced by the calculations, whereas bridging-bond lengths tend to be somewhat longer than the corresponding experimental results. In addition, it is worth noting that calculations predict that the M−O bond distances in Mo and W species are essentially equal, regardless of the molecular conformation of the anion.

Amado and Ribeiro-Claro[16] have recently reported computational results for a series of group 5−7 transition-metal $[M_2O_7]^{n-}$ systems and have suggested that linearity of the M−O−M bridging unit appears to be particularly favorable for V, Nb, and Ta (over group 6 and 7 elements) primarily as a consequence of stronger $\pi$-type M d−O p orbital interactions in these species, although some consideration was also given to the effect of the total charge of the oxoanions. In the present work, we have carried out detailed molecular-orbital and population analyses to gain insight into the influence of the electrostatic and bonding interactions on the molecular structures of the $[M_2O_7]^{n-}$ anions. The results obtained are discussed in the next two sections.

**Molecular-Orbital Analysis.** Eigenvalue diagrams for the occupied valence levels in $D_{3d}$ and $C_s$ conformers are shown in Figure 2. A comparison of absolute orbital eigenvalues is not possible due to the differences in the total charge of the systems. Therefore, molecular-orbital energies are given relative to a value of 0.0 eV assigned to the $1a_{2g}$ ($D_{3d}$) and 13a″ ($C_s$) orbitals, which constitute the highest-occupied level (HOMO) and are purely O p in character, in all species. Qualitative diagrams for $D_{3d}$ and $C_s$ species are shown in Figures 3 and 4, respectively. It should be noted that these molecular-orbital schemes are entirely qualitative, and no accurate quantitative correlation exists among the positions of the atomic and molecular energy levels. The diagrams are intended to summarize the most general and representative characteristics of the electronic structure of the oxoanion series studied, by highlighting the major atomic contributions to the molecular orbitals.

All the molecular-orbital diagrams possess a common (qualitative) characteristic in that they consist of two sets of energy

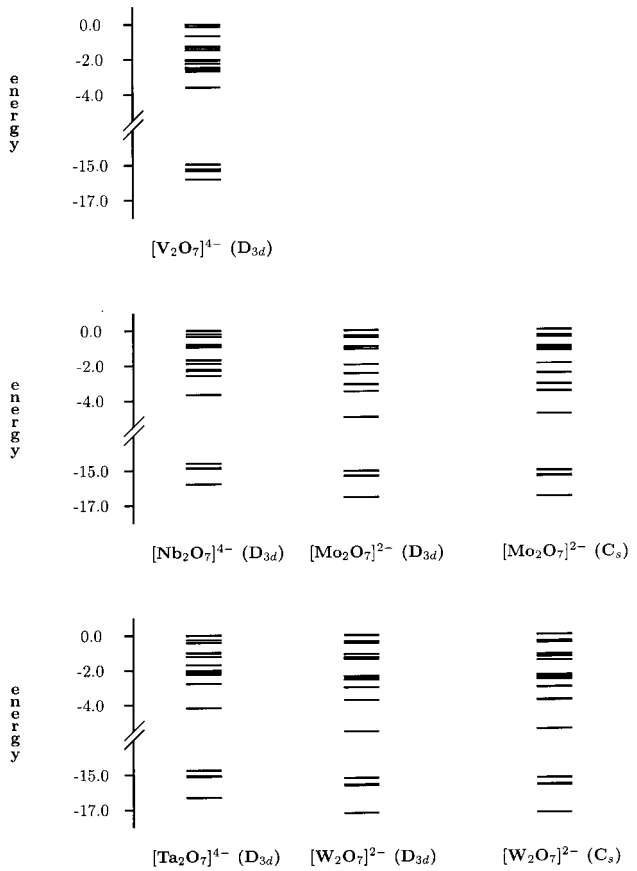


**Figure 2.** Eigenvalue (eV) diagram for occupied valence orbitals of systems with linear ($D_{3d}$) and bent ($C_s$) M−O−M bridging units.

levels, separated by a gap of about 10 eV. Only (quantitatively) small differences can be detected among the individual anions, mainly some stabilization of the orbital energies in Mo and W species with respect to those of the Nb and Ta systems, associated with the increase of the metal nuclear charge and decrease of the total molecular charge. In dimolybdates and ditungstates, the electronic structures of the different conformers are all (qualitatively and quantitatively) remarkably similar, whether the M−O−M bridge is linear or bent.

The orbitals comprising the low-lying set are predominantly of O s (both $O_b$ and $O_t$) character and, thus, are nonbonding. Two subsets can be distinguished in the high-lying group, although some overlap between them is observed, especially in the V, Nb, and Ta oxoanions. The higher-energy levels correspond to nonbonding combinations of p-type functions from $O_b$ and $O_t$ atoms, whereas the lower-energy levels are composed of orbitals incorporating significant contributions from both the metal and oxygen atoms, thus representing M−O bonding interactions.

Some details of the composition of the M−O bonding orbitals are given in Figures 3 and 4, and spatial electron-density plots for the orbitals involving the bridging-O atom are shown in Figures 5 and 6 for $D_{3d}$ and $C_s$ species, respectively (these plots correspond to Mo anions but are representative of all systems). All molecular orbitals in this subset possess M d and O p character, and there are no significant contributions from metal s or p orbitals, or from oxygen s-type functions. The lowest-lying orbital ($4a_{2u}$ ($D_{3d}$) and 12a′ ($C_s$)) describes a $\sigma$ bond over the M−O−M bridge, whereas the seven highest-lying orbitals represent interactions between the M and $O_t$ centers, with no appreciable $O_b$ contributions. The two remaining orbitals ($3e_u$

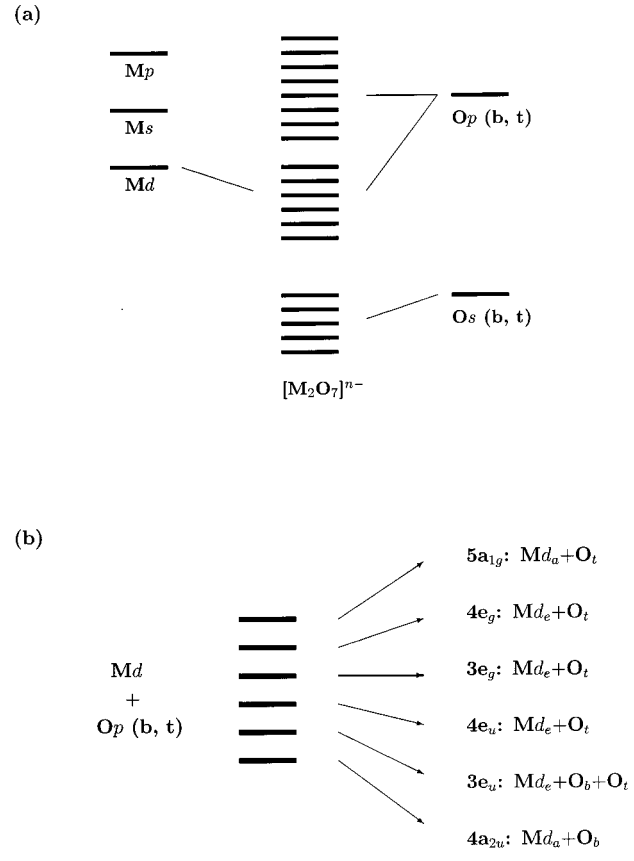


**Figure 3.** Qualitative molecular-orbital diagrams showing (a) predominant metal and oxygen contributions to the occupied valence orbitals of $D_{3d}$ conformers and (b) a more detailed description of the orbitals possessing substantial M and O character (for $d_a$, $d_{z^2}$; for $d_e$: $d_{x^2-y^2}$, $d_{xy}$, $d_{xz}$, $d_{yz}$).

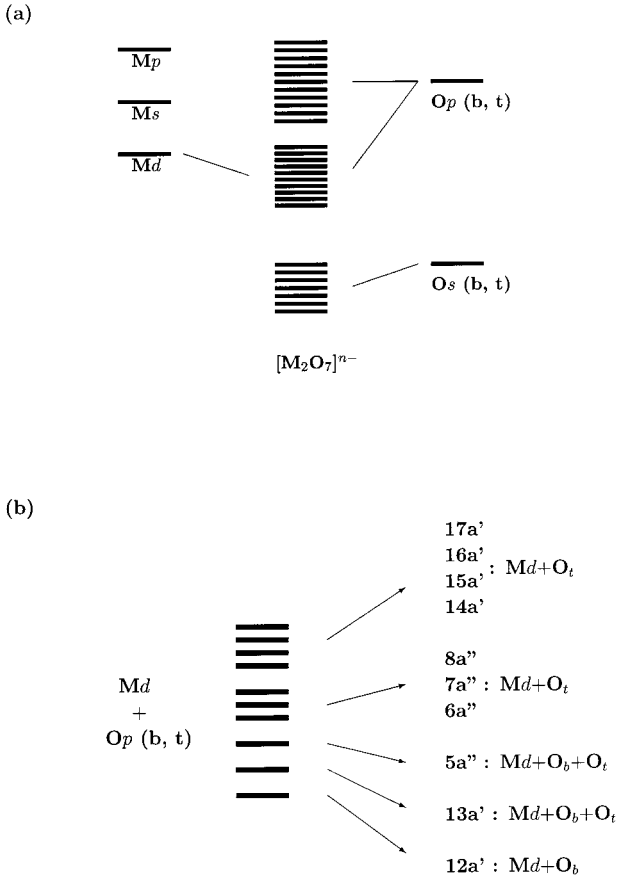


**Figure 4.** Qualitative molecular-orbital diagrams showing (a) predominant metal and oxygen contributions to the occupied valence orbitals of $C_s$ conformers and (b) a more detailed description of the orbitals possessing substantial M and O character.

($D_{3d}$), 13a′ and 5a″ ($C_s$)) correspond to the M−$O_b$−M $\pi$ bonds, but they are also substantially delocalized over the M−$O_t$ groups.

The M−O−M bridge can be described, in terms of molecular-orbital theory, as a three-center triple bond, and a bond order of 1.5 could in principle be ascribed to the individual M−$O_b$ interactions. Multiple-bonding character in the M−$O_t$ groups is also revealed by the molecular-orbital analysis. However, the bridging-bond lengths are considerably longer than the terminal-bond distances, and they are, in fact, more typical of a single M−O bond.[6] This point is discussed further in the next section.

**Population Analysis.** Results obtained from Mulliken and Mayer analyses are summarized in Tables 4−7. It is worth noting that, although these methods are known to exhibit basis-set dependence, (relative) Mulliken charges and Mayer bond indices can provide valuable chemical information for inorganic systems, if uniformity and consistency of the basis sets are maintained.[33] Furthermore, Mulliken analysis has been described as "not an arbitrary choice ... but consistent with the internal structure of the molecular-orbital formalism".[27]

Mulliken charges for metal and oxygen atoms are given in Table 4, where they are compared with the results from Voronoi analysis. The absolute charges are different, the latter being somewhat larger, but the relative values (the most useful chemical data) display a similar behavior. The populations of the metal basis functions have been calculated, for each type of orbital, by dividing the corresponding total percentage population by the number of orbitals, and are shown in Table 5. The almost exclusive participation of metal d orbitals in M−O bonding in the $[M_2O_7]^{n-}$ anions, evident in the results from the molecular-orbital analysis, is clearly shown by the population figures, the values per individual d-type function being, on average, 6 or 7 times greater than those for s and p orbitals. The Mulliken charges on the M atoms are all rather small, especially when compared with the formal oxidation states, and correspond to $d^3$ or $d^4$ electronic configurations for the metal centers (in contrast to the formal $d^0$ assignment).

Some trends are worthy of comment and can be summarized by noting that the charges on the metal atoms increase across a given row and downward in each group. The first trend reflects the increase in formal oxidation state, and has also been observed for $[MO_4]^{n-}$ anions of several transition metals.[32] However, the second trend contradicts the results of HF calculations on the Mo and W oxoanions.[12] This disagreement may simply be the consequence of computational effects associated with the basis-set dependence of Mulliken charges. Nevertheless, there is an important difference between these HF calculations and our DF approach, which lies in the explicit use of a relativistic treatment, included in the present work (via the ZORA method) but not in the HF investigation.[12] Thus, the higher charges on Ta and W (than on Nb and Mo) appear to correlate with changes in the populations of s and d orbitals (which increase and decrease, respectively) that can be related to the relativistic stabilization of the former and destabilization of the latter in 5d transition metals.[34] This reduction in Ta and W d-orbital populations (with respect to those of Nb and Mo) is greater than the increase in s-orbital populations and results in higher values for the Mulliken charges.

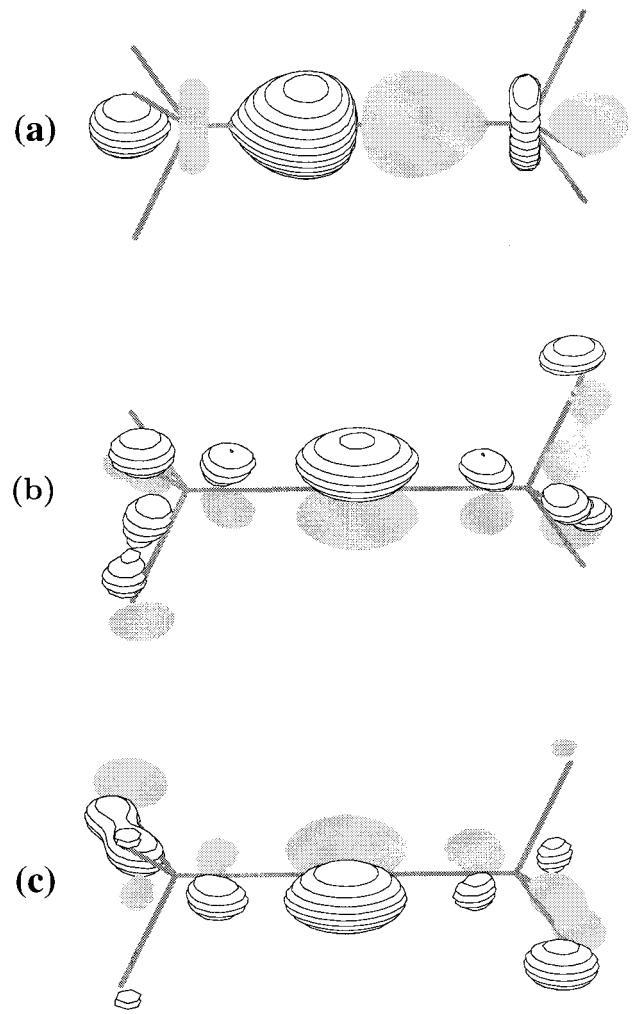


**Figure 5.** Spatial molecular-orbital representation of the (a) $\sigma$ ($4a_{2u}$ orbital) and (b) and (c) $\pi$ ($3e_u$ orbitals) M−O interactions involving the bridging-oxygen atom, in $D_{3d}$ conformers.

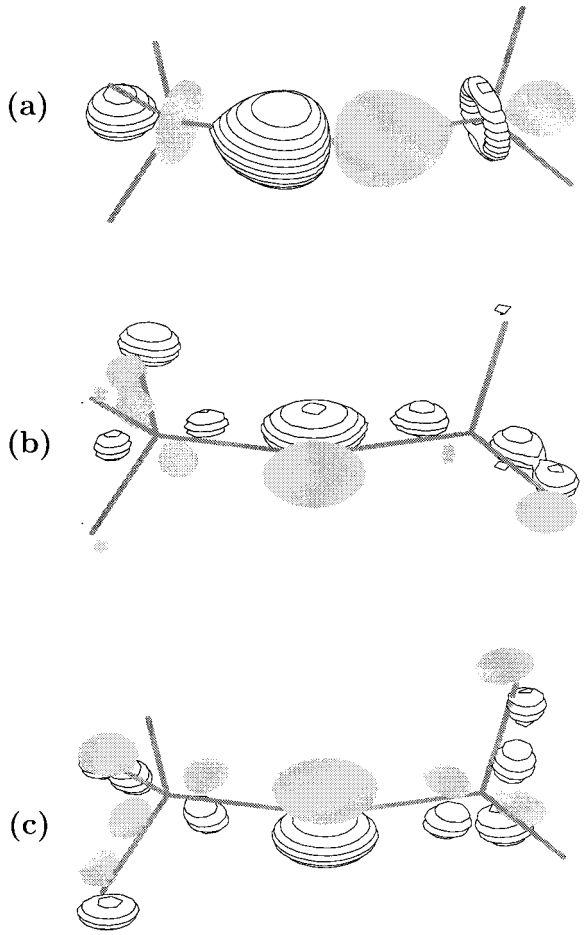


**Figure 6.** Spatial molecular-orbital representation of the (a) $\sigma$ (12a′ orbital) and (b) and (c), respectively, $\pi$ (12a′ and 5a″ orbitals) M−O interactions involving the bridging-oxygen atom, in $C_s$ conformers.

**TABLE 4: Mulliken and Voronoi Charges**

| | | Mulliken | | | Voronoi | | |
|---|---|---|---|---|---|---|---|
| molecule | symmetry | M | $O_b$ | $O_t$ | M | $O_b$ | $O_t$ |
| $[V_2O_7]^{4-}$ | $D_{3h}$, $D_{3d}$ | 1.40 | −0.94 | −0.98 | 2.02 | −1.13 | −1.15 |
| $[Nb_2O_7]^{4-}$ | $D_{3h}$, $D_{3d}$ | 1.46 | −1.02 | −0.98 | 2.78 | −1.41 | −1.36 |
| $[Ta_2O_7]^{4-}$ | $D_{3h}$, $D_{3d}$ | 1.58 | −1.03 | −1.02 | 2.93 | −1.46 | −1.40 |
| $[Mo_2O_7]^{2-}$ | $D_{3h}$, $D_{3d}$ | 1.87 | −0.98 | −0.79 | 2.96 | −1.31 | −1.10 |
| | $C_{2v}$, $C_2$, $C_s$ | 1.87 | −0.99 | −0.80 | 2.96 | −1.30 | −1.10 |
| $[W_2O_7]^{2-}$ | $D_{3h}$, $D_{3d}$ | 2.01 | −1.02 | −0.84 | 2.22 | −1.39 | −1.18 |
| | $C_{2v}$, $C_2$, $C_s$ | 2.01 | −1.02 | −0.84 | 3.21 | −1.38 | −1.17 |

**TABLE 5: Populations of Metal Basis Functions, Given as Percentage per Individual Orbital**

| molecule | symmetry | s | p | d |
|---|---|---|---|---|
| $[V_2O_7]^{4-}$ | $D_{3h}$, $D_{3d}$ | 1.9 | 3.4 | 17.6 |
| $[Nb_2O_7]^{4-}$ | $D_{3h}$, $D_{3d}$ | 2.0 | 3.3 | 17.6 |
| $[Ta_2O_7]^{4-}$ | $D_{3h}$, $D_{3d}$ | 5.8 | 2.9 | 17.1 |
| $[Mo_2O_7]^{2-}$ | $D_{3h}$, $D_{3d}$ | 0.0 | 2.3 | 18.6 |
| | $C_{2v}$, $C_2$, $C_s$ | 0.0 | 2.3 | 18.6 |
| $[W_2O_7]^{2-}$ | $D_{3h}$, $D_{3d}$ | 3.5 | 2.3 | 17.9 |
| | $C_{2v}$, $C_2$, $C_s$ | 3.5 | 2.3 | 17.9 |

The Mulliken charges on the $O_b$ atoms are similar in all systems, and those on the $O_t$ atoms are about 0.2 units smaller for the Mo and W anions than they are for the Nb and Ta species (a natural-population analysis of $D_{3d}$ dimolybdates and ditunsgates has yielded similar relative O charges[12]). These results indicate that the excess negative charge in the latter appears to accumulate on the two terminal $O_3$ groupings, and therefore suggest that the electrostatic repulsion between them should be an important factor in the apparently strong preference for linear-bridge conformations shown by the Nb and Ta dimetalates. Mayer bond orders are given in Table 6, and an analysis of the different orbital contributions to the indices for bridging bonds, grouped by symmetry types, is presented in Table 7. Also included in Table 6 is a comparison between the Mayer values and the results obtained with a bond-valence model based on the following relationship[6]

$$\log s = (d_0 - d)^B$$

where $s$ is the bond valence, $d_0$ is the single-bond length, $B$ defines the slope of the bond length−bond valence functions, and $d$ is a calculated bond distance. In general, the Mayer values are in good agreement with those from the classical model. All results lie within the typically observed deviation range of 0.2−0.3 units from bond-valence values, the largest differences occurring in terminal Nb−O and Ta−O bonds, and bridging Mo−O and W−O bonds.

The Mayer indices clearly show the multiple-bonding character of terminal bonds, but not of bridging bonds, in accordance with the significant differences observed between M−$O_b$ and M−$O_t$ distances. Although the molecular-orbital analysis reveals multiple bonds between M and $O_b$ atoms, the orbitals corresponding to $\pi$ interactions along the M−O−M moiety extend

**TABLE 6: Mayer Indices for Bridging and Terminal M−O Bonds**[a]

| molecule | symmetry | M−$O_b$ | | M−$O_t$ | |
|---|---|---|---|---|---|
| $[V_2O_7]^{4-}$ | $D_{3d}$ | 0.75 | (0.85) | 1.44 | (1.27) |
| $[Nb_2O_7]^{4-}$ | $D_{3d}$ | 0.72 | (0.80) | 1.49 | (1.20) |
| $[Ta_2O_7]^{4-}$ | $D_{3d}$ | 0.76 | (0.81) | 1.50 | (1.18) |
| $[Mo_2O_7]^{2-}$ | $D_{3d}$ | 0.68 | (1.04) | 1.55 | (1.49) |
| | $C_s$ | 0.68 | (1.01) | 1.55 | (1.49) |
| $[W_2O_7]^{2-}$ | $D_{3d}$ | 0.72 | (1.01) | 1.59 | (1.43) |
| | $C_s$ | 0.72 | (1.01) | 1.60 | (1.43) |

[a] Values in parentheses are results from classical bond-valence analysis.

**TABLE 7: Bond-Order Index Decomposition for Bridging Bonds**

| symmetry | molecule | bond order | decomposition | |
|---|---|---|---|---|
| $D_{3d}$ | | | $(a_{1g}+)\ a_{2u}$ | $e_u$ |
| | $[V_2O_7]^{4-}$ | 0.75 | 0.33 | 0.42 |
| | $[Nb_2O_7]^{4-}$ | 0.72 | 0.36 | 0.36 |
| | $[Ta_2O_7]^{4-}$ | 0.76 | 0.41 | 0.35 |
| | $[Mo_2O_7]^{2-}$ | 0.68 | 0.36 | 0.32 |
| | $[W_2O_7]^{2-}$ | 0.72 | 0.42 | 0.30 |
| $C_s$ | | | a′ | a″ |
| | $[Mo_2O_7]^{2-}$ | 0.68 | 0.52 | 0.16 |
| | $[W_2O_7]^{2-}$ | 0.72 | 0.57 | 0.15 |

over the whole molecular structure, and the small value of the M−$O_b$ bond order indicates that this extensive delocalization of the electron density must have an important weakening effect on the bonding along the bridging unit, which is observed through (unexpectedly) long M−$O_b$ bonds.

For the species with a linear bridge, it is possible to separate the $\sigma$ and $\pi$ contributions to M−$O_b$ bonds by calculating $a_{2u}$ and $e_u$ indices, respectively (in order to ensure that the partial values add up to the total bond order, small contributions to the $\sigma$ index have to be included, and this is represented as $(a_{1g}+)$ $a_{2u}$ in Table 7). The results obtained for the $e_u$ index agree with the suggestion that the conformations with a linear bridge are preferred by group 5 elements due to more favorable $\pi$-type interactions between metal *d* and bridging-oxygen p orbitals. However, the differences between the two groups are small, and it is therefore likely that the repulsions between the terminal $O_3$ groupings may be as, or even more, important as the orbital interactions in determining the structural preferences. A factor that seems to reinforce the effect of repulsive interactions is found in the identical bond-order results for the $D_{3d}$ and $C_s$ conformers of the Mo and W anions (it should be noted that both total and partial values are identical, as the correspondence between the symmetry types is $a_{2u}$, a′ and $e_u$, a′ + a″). This suggests that the M−$O_b$ bonding interactions in these species are largely unaffected by bending.

## Conclusion

The molecular and electronic structures of the $[M_2O_7]^{n-}$ anions of V, Nb, Ta, Mo, and W have been studied by density-functional methods. Among the possible conformations investigated, only those exhibiting a linear M−O−M bridge have been found for V, Nb, and Ta, and although they have also been calculated to be the lowest-energy configurations for Mo and W, in these cases, the species with linear bridging units are only slightly more stable than those possessing a bent M−O−M moiety.

The molecular-orbital analysis has indicated that all M−O interactions possess M d−O p character, and that multiple bonds are formed between the metal and both bridging and terminal oxygen atoms. The multiple-bonding nature of M−$O_t$ interactions has been confirmed by the bond-order values obtained. However, possibly due to a weakening effect associated with electron delocalization, M−$O_b$ interactions are characterized by bond lengths and bond orders that are typical of a single M−O bond.

The results from population analysis (Mulliken charges and Mayer bond indices) have revealed that most of the negative charge in the oxoanions resides on the terminal $O_3$ groupings and that bending of the M−O−M bridge does not appear to affect the nature of the M−$O_b$ bonds. These observations have led us to the conclusion that repulsive interactions between the ends of the molecules may play a more important role in determining the structural preferences observed for the oxoanions than M−$O_b$ $\pi$ bonding does.

**Acknowledgment.** We thank EPSRC, the Cambridge Overseas Trust, Selwyn College (Cambridge), and the University of Hull for financial support, and the Computational Chemistry Working Party for access to computational facilities in the Rutherford Appleton Laboratory.

## References and Notes

(1) Pope, M. T. *Heteropoly and Isopoly Oxometalates*; Springer-Verlag: Heidelberg, 1983.
(2) Pope, M. T.; Müller, A. *Angew. Chem., Int. Ed. Engl.* **1991**, *30*, 34.
(3) Baker, L. C. W.; Glick, D. C. *Chem. Rev.* **1998**, *98*, 3.
(4) Pope, M. T., Müller, A., Ed. *Polyoxometalates: from Platonic Solids to Anti-retroviral Activity*; Kluwer: Dordrecht, The Netherlands, 1994.
(5) Calvo, C.; Faggiani, R. *Acta Crystallogr. B* **1975**, *31*, 603.
(6) Tytko, K. H.; Mehmke, J.; Fischer, S. *Struct. Bonding* **1999**, *93*, 129.
(7) Day, V. M.; Fredich, M. F.; Klemperer, W. G.; Shum, W. *J. Am. Chem. Soc.* **1977**, *99*, 6146.
(8) Braunstein, P.; deMéricdeBellefon, C.; Lanfranchi, M.; Tiripicchio, A. *Organometallics* **1984**, *3*, 1772.
(9) Bhattacharyya, R. G.; Biswas, S. *Inorg. Chim. Acta* **1991**, *181*, 213.
(10) Boukhari, A. *J. Alloys Compounds* **1992**, *188*, 14.
(11) Lynton, H.; Truter, M. R. *J. Chem. Soc.* **1960**, 5112.
(12) Mestres, J.; Duran, M.; Martín-Zarza, P.; MedinadelaRosa, E.; Gili, P. *Inorg. Chem.* **1993**, *32*, 4708.
(13) Ozeki, T.; Kinoshita, Y.; Adachi, H.; Ikeda, S. *Bull. Chem. Soc. Jpn.* **1994**, *67*, 1041.
(14) Brito, F.; Ascanio, J.; Mateo, S.; Hernández, C.; Araujo, L.; Gili, Martín-Zarza, P.; P.; Domínguez, S.; Mederos, A. *Polyhedron* **1997**, *16*, 3835.
(15) Ribeiro-Claro, P. J. A.; Amado, A. M.; Teixeira-Dias, J. J. C. *J. Comput. Chem.* **1996**, *17*, 1183.
(16) Amado, A. M.; Ribeiro-Claro, P. J. A. *THEOCHEM* **1999**, *469*, 191.
(17) ADF2000.02. Baerends, E. J.; Ellis, D. E.; Ros, P. *Chem. Phys.* **1973**, *2*, 41. Versluis, L.; Ziegler, T. *J. Chem. Phys.* **1988**, *322*, 88. teVelde, G.; Baerends, E. J. *J. Comput. Phys.* **1992**, *99*, 84. FonsecaGuerra, C.; Snijders, J. G.; teVelde, G.; Baerends, E. J. *Theor. Chem. Acc.* **1998**, *99*, 391.
(18) GAMESS-UK. A package of ab initio programs written by M. F. Guest, J. H. vanLenthe, J. Kendrick, K. Schoffel, P. Sherwood, with contributions from R. D. Amos, R. J. Buenker, M. Dupuis, N. C. Handy, I. H. Hillier, P. J. Knowles, V. Bonacic-Koutecky, W. von Niessen, R. J. Harrison, A. P. Rendell, V. R. Saunders, and A. J. Stone.
(19) Vosko, S. H.; Wilk, L.; Nusair, M. *Can. J. Phys.* **1980**, *58*, 1200.
(20) Kohn, W.; Sham, L. J. *Phys. Rev.* **1965**, *140*, A1133.
(21) Becke, A. D. *Phys. Rev. A* **1988**, *38*, 3098.
(22) Perdew, J. P. *Phys. Rev. B* **1986**, *33*, 8822.
(23) Stephens, P. J.; Devlin, F. J.; Chabalowski, C. F.; Frisch, M. J. *J. Phys. Chem.* **1994**, *98*, 11623.
(24) Stevens, W. J.; Basch, H.; Krauss, M. *J. Chem. Phys.* **1984**, *81*, 6026.
(25) Stevens, W. J.; Jasien, P. G.; Krauss, M.; Basch, H. *Can. J. Chem.* **1992**, *70*, 612.
(26) Cundari, T. R.; Stevens, W. J. *J. Chem. Phys.* **1993**, *98*, 5555.
(27) Mayer, I. *Chem. Phys. Lett.* **1983**, *97*, 270.
(28) Mayer, I. *Int. J. Quantum Chem.* **1984**, *26*, 151.
(29) MAYER. A program to calculate Mayer bond-order indices from

the output of the electronic structure packages GAMESS, GAUSSIAN, and ADF, written by A. J. Bridgeman, University of Hull 2001. Available from the author on request.

(30) Schaftenaar, G.; Noordik, J. H. MOLDEN. A pre- and postprocessing program for molecular and electronic structures. *J. Comput. Aided Mol. Design* **2000**, *14*, 123.

(31) Kohn, W.; Becke, A. D.; Parr, R. G. *J. Phys. Chem.* **1996**, *100*, 12974.

(32) Bridgeman, A. J.; Cavigliasso, G. *Polyhedron*, in press.

(33) Bridgeman, A. J.; Cavigliasso, G.; Ireland, L. R.; Rothery, J. *J. Chem. Soc., Dalton Trans.*, in press.

(34) Kaltsoyannis, N. *J. Chem. Soc., DaltonTrans.* **1997**, 1.

(35) Dorm, E.; Marinder, B. *Acta Chem. Scand.* **1967**, *21*, 590.

(36) Au, P. K. L.; Calvo, C. *Can. J. Chem.* **1967**, *45*, 2297.

(37) Kato, K.; Takayama-Muromachi, E. *Acta Crystallogr. C* **1985**, *41*, 1413.